Near Infrared Luminescence and Supramolecular Structure of a Helical Triple-Decker Yb(III) Schiff Base Cluster

5 AUTHORS, INCLUDING:

Michael Oye
University of California, Santa Cruz
39 PUBLICATIONS **690** CITATIONS

SEE PROFILE

Wai-Kwok Wong
Hong Kong Baptist University
239 PUBLICATIONS **4,704** CITATIONS

SEE PROFILE

Near Infrared Luminescence and Supramolecular Structure of a Helical Triple-Decker Yb(III) Schiff Base Cluster

Xiao-Ping Yang,[†] Richard A. Jones,*,[†] Michael M. Oye,[‡] Archie L. Holmes,[‡] and Wai-Kwok Wong*,[#]

Department of Chemistry and Biochemistry, The University of Texas at Austin, 1 University Station A5300, Austin, Texas, 78712-0165, Microelectronics Research Center and Texas Materials Institute, The University of Texas at Austin, 1 University Station Stop R9900, Austin, Texas, 78712-0165, Chemistry Department, Hong Kong Baptist University, Kowloon Tong, Hong Kong, P. R. China

ABSTRACT: The triple-decker complex $[Yb_3L_3(OAc)_2Cl](H_2O)_3(CH_3OH)_{1.5}(CH_3CN)_{0.5}$ (**1**) is formed from the reaction of H_2L, $YbCl_3 \cdot 6H_2O$, and $Zn(OAc)_2 \cdot 2H_2O$ in 25% yield (H_2L = N,N'-bis(5-bromo-3-methoxysalicylidene)phenylene-1,2-diamine). The single-crystal X-ray structure of **1** revealed the presence of two independent, chiral molecules of **1** in the asymmetric unit. Intermolecular $\pi-\pi$ stacking and $C-H\cdots\pi$ interactions between both sets of Yb_3L_3 units create two one-dimensional strands, A and B. Strands of A are cross-linked via $Br\cdots H-C$ hydrogen bonds creating a three-dimensional network that encloses the B strands. Near-infrared (NIR) lanthanide luminescence in both the solid state and the solution is observed in **1**.

Introduction

Luminescent polynuclear lanthanide complexes are currently of interest for potential application in biology, medicine, and materials science.[1] Recently, attention has been focused on complexes of Yb(III), Nd(III), and Er(III), which are capable of emission in the near-infrared (NIR) since they have the potential to be used as stains for immunoassays or for the imaging of cells using time-resolved luminescence.[2] The photophysical properties of lanthanide ions are markedly dependent on their environment. For efficient emissions, chromophoric ligands are often employed to transfer absorbed energy efficiently to the lanthanide ions (the "antenna" effect). Such ligands can also protect the Ln(III) center from solvent molecules which can quench emissions. Many multidentate cyclic and acyclic ligands designed to encapsulate lanthanides are now known.[3] They include cryptand, calixarene, cyclodextrin, podand-type, and terpyridine-like ligands, which have been mostly used with Tb(III) and Eu(III) ions to produce luminescence in the visible region. As part of a study focused on the design and synthesis of new polynuclear lanthanide complexes, we recently described the synthesis, structures, and photophysical properties of both "tetra-decker" and "triple-decker" Tb-(III) complexes derived from the salen-like Schiff base N,N'-bis(5-bromo-3-methoxysalicylidene)phenylene-1,2-diamine (H_2L).[4] The multidecker frameworks of these complexes feature extensive $\pi-\pi$ interactions between aromatic groups that enclose the three Tb(III) ions in a stacked helical fashion and help to shield them from solvent and water molecules. We have now extended our studies of multidecker lanthanide complexes and describe here the synthesis, structure, and photophysical properties of the triple-decker complex $[Yb_3L_3(OAc)_2Cl]$ (**1**). In the solid state, **1** exhibits an unusual multistrand supramolecular architecture.

* To whom correspondence should be addressed. (R.A.J.) Tel: (512) 471-1706. E-mail: rajones@mail.utexas.edu. (W.-K.W.) Tel: +852 3411 7075. Fax: +852 3411 7348. E-mail: wkwong@hkbu.edu.hk.
    † Department of Chemistry and Biochemistry, The University of Texas at Austin.
    ‡ Microelectronics Research Center and Texas Materials Institute, The University of Texas at Austin.
    # Hong Kong Baptist University.

Experimental Section

General Methods. All reactions were performed under dry oxygen-free dinitrogen atmospheres using standard Schlenk techniques. $YbCl_3 \cdot 6H_2O$, $Zn(OAc)_2 \cdot 2H_2O$, acetonitrile, methanol, and diethyl ether were purchased from Aldrich. Solvents for photophysical investigations were dried over fresh 4A molecular sieves and freshly distilled under dry nitrogen before use. The Schiff base H_2L was prepared as previously described.[4,5] Physical measurements: Mass spec: ESI and FAB; Finnigan MAT TSQ 700; IR: Nicolet IR 200 FTIR spectrometer. UV−Vis: Beckman DU 640 spectrophotometer. Photoluminescence measurements were made at room temperature with a one-meter SPEX 1704 spectrometer and a liquid-nitrogen cooled Ge detector. The excitation was provided by an argon ion laser using either the UV multiline optics (333.6−363.8 nm range) or the laser line at 275.4 nm laser line. Melting points were obtained in sealed glass capillaries under dinitrogen and are uncorrected.

X-ray Crystallography. Data were collected on a Nonius Kappa CCD diffractometer with graphite monochromated Mo−Kα radiation (λ = 0.71073 Å) at 153 K. The absorption corrections was applied using GAUSSIAN. The structure was solved by direct methods and refined anisotropically using full-matrix least-squares methods with the SHELX 97 program package.[6] The coordinates of the non-hydrogen atoms were refined anisotropically, while hydrogen atoms were included in the calculation isotropically but not refined. Neutral atom scattering factors were taken from Cromer and Waber.[7]

Synthesis of $[Yb_3L_3(OAc)_2Cl](H_2O)_3(CH_3OH)_{1.5}(CH_3CN)_{0.5}$ (1). A solution of $YbCl_3 \cdot 6H_2O$ (0.077 g, 0.20 mmol) in MeOH (5 mL) was added to a solution of H_2L (0.107 g, 0.20 mmol) in MeCN (20 mL). The mixture was stirred and heated under reflux (5 min.). During this time, the color of the reaction mixture changed from red to yellow. A solution of $Zn(OAc)_2 \cdot 2H_2O$ (0.043 g, 0.20 mmol) in MeOH (5 mL) was added, and the resulting mixture was stirred and heated under reflux (20 min.). The mixture was then allowed to cool to room temperature and filtered. Diethyl ether was allowed to diffuse slowly into the filtrate at room temperature. Single crystals of **1** were collected by filtration after 4 weeks. Yield 0.040 g (25%), mp > 300 °C (dec), ESI-MS (CH₃-CN) m/z (%): 868 (40) $[M-L-3H_2O-1.5CH_3OH-0.5CH_3CN]^{2+}$. IR (CH₃-CN, cm⁻¹): 3377 (s), 2980 (m), 1642 (s), 1637 (s), 1560 (m), 1537 (m), 1452 (m), 1245 (m), 1058 (m), 747 (s), 620 (m), 579 (m).

Results and Discussions

Reaction of the Schiff base H_2L with $YbCl_3 \cdot 6H_2O$ and Zn-$(OAc)_2 \cdot 2H_2O$ in a 1:1:1 molar ratio in MeCN/MeOH (2:1) produces the triple-decker complex $[Yb_3L_3(OAc)_2Cl]$ (**1**) in 25% overall yield. Single crystals of **1** suitable for X-ray diffraction

(a)

(b)

Figure 1. View of the two independent molecules of **1** ((a) Δ[a], (b) Λ[b]) present in the asymmetric unit.

Table 1. Selected Bond Lengths (Å) and Angles (°) for 1

Yb(3)−O(3C)	2.262(3)	O(2C)−Yb(2)−O(3C)	66.95(9)
Yb(3)−O(6)	2.292(3)	O(5)−Yb(2)−O(3B)	95.89(10)
Yb(3)−O(2C)	2.311(3)	O(2C)−Yb(2)−O(3B)	158.94(9)
Yb(3)−O(7)	2.383(4)	O(3C)−Yb(2)−O(3B)	133.49(9)
Yb(3)−O(8)	2.402(3)	O(5)−Yb(2)−O(2B)	85.16(11)
Yb(3)−O(1C)	2.566(3)	O(2C)−Yb(2)−O(2B)	92.04(9)
Yb(3)−Cl(1)	2.5826(14)	O(3C)−Yb(2)−O(2B)	155.87(9)
Yb(3)−O(4C)	2.584(3)	O(3B)−Yb(2)−O(2B)	68.94(9)
Yb(2)−O(5)	2.265(3)	O(5)−Yb(2)−N(1C)	155.53(11)
Yb(2)−O(2C)	2.277(2)	O(2C)−Yb(2)−N(1C)	72.24(11)
Yb(2)−O(3C)	2.283(3)	O(3C)−Yb(2)−N(1C)	105.16(11)
Yb(2)−O(3B)	2.292(3)	O(3B)−Yb(2)−N(1C)	94.16(10)
Yb(2)−O(2B)	2.334(3)	O(2B)−Yb(2)−N(1C)	77.75(11)
Yb(2)−N(1C)	2.467(4)	O(5)−Yb(2)−N(2C)	139.70(11)
Yb(2)−N(2C)	2.498(4)	O(2C)−Yb(2)−N(2C)	105.89(11)
Yb(2)−O(4B)	2.738(3)	O(3C)−Yb(2)−N(2C)	70.81(11)
Yb(1)−O(2A)	2.208(3)	O(3B)−Yb(2)−N(2C)	81.11(11)
Yb(1)−O(3A)	2.217(3)	O(2B)−Yb(2)−N(2C)	129.06(11)
Yb(1)−O(3B)	2.297(3)	N(1C)−Yb(2)−N(2C)	64.02(12)
Yb(1)−O(2B)	2.384(3)	O(5)−Yb(2)−O(4B)	68.28(10)
Yb(1)−N(1B)	2.464(4)	O(2C)−Yb(2)−O(4B)	139.81(9)
Yb(1)−N(2A)	2.470(4)	O(3C)−Yb(2)−O(4B)	76.39(9)
Yb(1)−N(1A)	2.487(4)	O(3B)−Yb(2)−O(4B)	60.84(9)
Yb(1)−N(2B)	2.534(4)	O(2B)−Yb(2)−O(4B)	118.73(9)
O(3C)−Yb(3)−O(6)	86.12(11)	N(1C)−Yb(2)−O(4B)	135.62(11)
O(3C)−Yb(3)−O(2C)	66.71(9)	N(2C)−Yb(2)−O(4B)	75.58(10)
O(6)−Yb(3)−O(2C)	83.54(11)	O(2A)−Yb(1)−O(3A)	74.94(11)
O(3C)−Yb(3)−O(7)	82.60(11)	O(2A)−Yb(1)−O(3B)	146.37(11)
O(6)−Yb(3)−O(7)	150.83(11)	O(3A)−Yb(1)−O(3B)	138.36(10)
O(2C)−Yb(3)−O(7)	115.85(13)	O(2A)−Yb(1)−O(2B)	139.70(9)
O(3C)−Yb(3)−O(8)	109.89(12)	O(3A)−Yb(1)−O(2B)	78.44(10)
O(6)−Yb(3)−O(8)	154.01(11)	O(3B)−Yb(1)−O(2B)	68.00(9)
O(2C)−Yb(3)−O(8)	84.35(11)	O(2A)−Yb(1)−N(1B)	78.14(11)
O(7)−Yb(3)−O(8)	54.51(11)	O(3A)−Yb(1)−N(1B)	93.58(12)
O(3C)−Yb(3)−O(1C)	129.47(9)	O(3B)−Yb(1)−N(1B)	99.81(11)
O(6)−Yb(3)−O(1C)	82.64(11)	O(2B)−Yb(1)−N(1B)	73.90(10)
O(2C)−Yb(3)−O(1C)	63.15(9)	O(2A)−Yb(1)−N(2A)	108.29(12)
O(7)−Yb(3)−O(1C)	124.88(10)	O(3A)−Yb(1)−N(2A)	73.05(12)
O(8)−Yb(3)−O(1C)	71.38(11)	O(3B)−Yb(1)−N(2A)	83.85(12)
O(3C)−Yb(3)−Cl(1)	144.55(7)	O(2B)−Yb(1)−N(2A)	91.88(10)
O(6)−Yb(3)−Cl(1)	86.53(9)	N(1B)−Yb(1)−N(2A)	162.40(11)
O(2C)−Yb(3)−Cl(1)	146.29(7)	O(2A)−Yb(1)−N(1A)	72.08(11)
O(7)−Yb(3)−Cl(1)	87.25(10)	O(3A)−Yb(1)−N(1A)	112.29(12)
O(8)−Yb(3)−Cl(1)	90.94(9)	O(3B)−Yb(1)−N(1A)	86.52(11)
O(1C)−Yb(3)−Cl(1)	83.69(7)	O(2B)−Yb(1)−N(1A)	147.28(10)
O(3C)−Yb(3)−O(4C)	63.69(9)	N(1B)−Yb(1)−N(1A)	132.86(12)
O(6)−Yb(3)−O(4C)	78.02(11)	N(2A)−Yb(1)−N(1A)	64.26(12)
O(2C)−Yb(3)−O(4C)	127.81(9)	O(2A)−Yb(1)−N(2B)	80.42(12)
O(7)−Yb(3)−O(4C)	72.86(11)	O(3A)−Yb(1)−N(2B)	149.15(11)
O(8)−Yb(3)−O(4C)	127.09(12)	O(3B)−Yb(1)−N(2B)	69.30(11)
O(1C)−Yb(3)−O(4C)	155.85(12)	O(2B)−Yb(1)−N(2B)	110.78(11)
Cl(1)−Yb(3)−O(4C)	80.85(7)	N(1B)−Yb(1)−N(2B)	63.02(11)
O(5)−Yb(2)−O(2C)	91.22(10)	N(2A)−Yb(1)−N(2B)	133.45(11)
O(5)−Yb(2)−O(3C)	83.65(11)	N(1A)−Yb(1)−N(2B)	76.44(12)

studies were obtained by allowing Et₂O to diffuse into the reaction mixture at room temperature. The complex crystallizes in the triclinic space group P$\bar{1}$ with two similar but independent molecules (a and b) in the asymmetric unit, giving four molecules, two pairs of enantiomers per unit cell (Figure 1). The metric parameters of the two independent molecules are similar (Table 1). For example, in a, Yb(1)−Yb(2) = 3.838 Å and Yb(2)−Yb(3) = 3.692 Å. Each Yb(III) ion is eight-coordinate with Yb(1) bound by the N₂O₂ donor sets of two L groups. One of these groups is essentially sandwiched between Yb(1) and Yb(2) with the two phenolic oxygen atoms of this ligand also bridging the two metals. Yb(2) is further coordinated by the oxygen atoms of a phenolic OMe group, by the N₂O₂ donor sets of the third L group, and by the oxygen atom of an acetate unit that bridges Yb(2)−Yb(3). The coordination geometry of Yb(3) is completed by two bridging phenolic oxygen atoms of the third L group, two phenolic OMe groups, a terminal chloride, a chelating acetate, and an oxygen atom of the μ-OAc group. The aryl units display extensive intramolecular π−π stacking interactions, which may further add to the stability of the compound. As shown in Figure 1, the three Schiff base

ligands enclose the central Yb₃ core in a chiral helical fashion. The two independent molecules in the unit cell have opposite directions of twist. We assign the Δ[a] designation to the molecule a since when viewed from Yb(1) to Yb(3) the L groups appear to deflect in a clockwise fashion. In the second molecule (b), the deflection is anticlockwise (Λ[b]). The unit cell therefore contains two pairs of enantiomers (Δ[a] Λ[a] and Λ[b] Δ[b]) formed by the symmetry operation required by the P$\bar{1}$ space group. The extended solid-state structure of **1** is noteworthy since it features extensive supramolecular interactions which are different for the two sets of molecules. For a-type molecules (Yb(1)−Yb-(2)−Yb(3)) intermolecular π−π stacking and C−H···π interactions form extended one-dimensional (1D) strands (A) (···Δ[a]−Λ[a]−Δ[a]−Λ[a]···) (Figure 2). For b-type molecules the Yb₃L₃ units form a supramolecular 1D strands (B) via intramolecular π−π stacking interactions (Figure 3). The two strands also pack differently. Strands of type A are further cross-linked with each other by hydrogen bonded interactions between Br and C−H···· of a salen methoxy group (Figure 4) (Br···H−C 2.943 and 3.052 Å) resulting in a three-dimensional network. The B strands
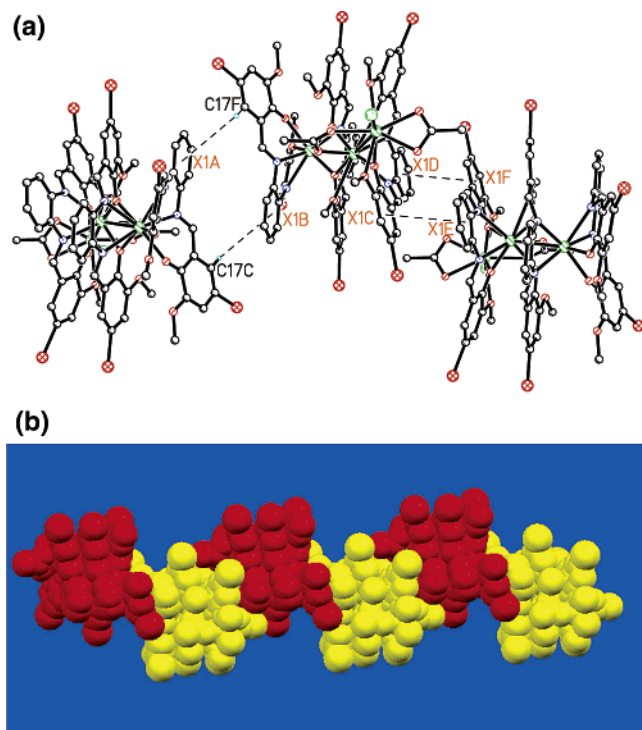
(a)

(b)

Figure 2. (a) Intermolecular $\pi-\pi$ stacking and C−H···π interactions in A strands. (X1C(D)···X1E(F): 3.891 Å and H(17F)···π: 3.208 Å, C−H−π: 131.1°). (b) Space filling model of the 1-D strand A (red: $\triangle$; yellow: Λ).
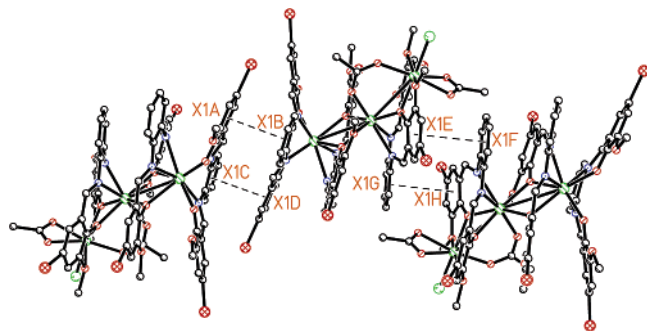

Figure 3. Intermolecular $\pi-\pi$ stacking interactions in B strands. (X1A-(C)···X1B(D): 3.677 Å, X1E(G)···X1F(H): 3.927 Å).

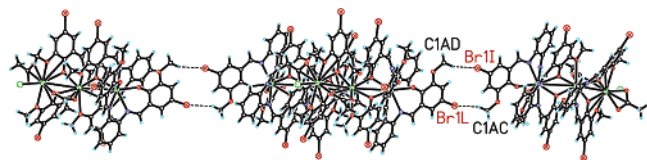**Figure 4.** Cross-linking of A strands via C−H···Br interactions. (H(1AD)···Br(1J): 2.943 Å, C(1AD)···Br(1J): 3.629 Å, C−H−Br: 129.5°).

are not interconnected with each other but are simply enclosed within the network structure created by the A strands. Figure 5 illustrates this feature with a view along the *a*-axis. It is interesting to note that **1** adopts this complex supramolecular structure. In contrast, the Tb analogue of **1**, [Tb$_3$L$_3$(OAc)$_2$Cl], crystallizes in the monoclinic space group $P2(1)/n$ with one molecule per asymmetric unit. In this case, the molecules are further connected by intermolecular $\pi-\pi$ stacking interactions resulting in only one type of simple 1-D strand (Figure S1, Supporting Information).
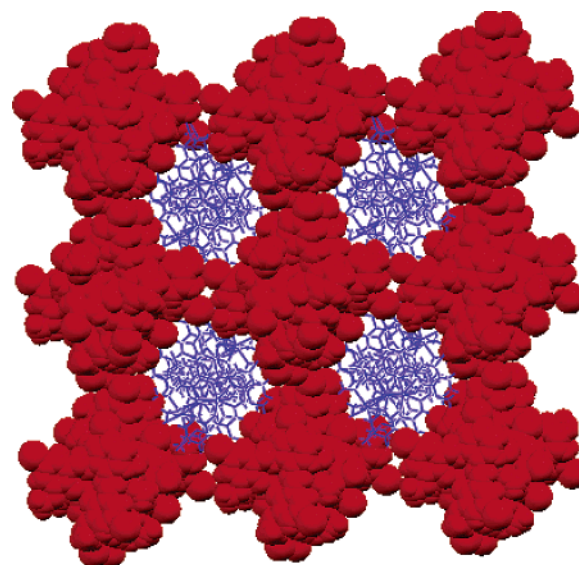

Figure 5. View of **1** along the *a*-axis showing incorporation of the B strands (blue) by the A strands (red).
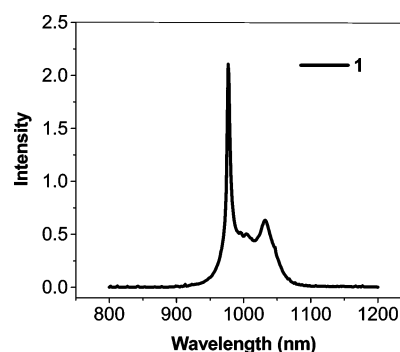

Figure 6. The NIR luminescence of **1** in CH$_3$CN (2.0×10^{-6} M).

We have studied the NIR luminescence properties of **1** in MeCN, CD$_3$OD, and CH$_3$OH. In MeCN, the typical emission band of Yb^{3+} assigned to the $^2F_{5/2} \rightarrow {}^2F_{7/2}$ transitions is observed at 976 nm upon excitation of the ligand-centered absorption band either at 275 or 333−363 nm (Figure 6). A similar NIR luminescence is also observed for **1** in the solid state. The free ligand H$_2$L does not exhibit NIR luminescence under similar conditions. Molar conductivity studies of **1** indicate that the molecule does not dissociate in MeCN solution, while in MeOH there appears to be some degree of decomposition. These observations are consistent with the NIR luminescence of **1** in MeCN solution coming from a trimetallic Yb(III) complex with a structure similar to that found in the solid state. **1** shows weaker NIR luminescence intensity in CD$_3$OD, and it is hardly detected in CH$_3$OH. These observations could be due to a strong interaction between **1** and CH$_3$OH which may lead to some decomposition. We were interested in comparing the emission intensities of **1** with related complexes that contain both Yb-(III) ions and the same ligand (L). Although the simple heterodinuclear 3d−4f complex [ZnYbL(OAc)(NO$_3$)$_2$] (**2**)[4] is not completely analogous to **1**, it does provide an example of compound containing L and Yb(III). Using solutions with their concentrations adjusted to give the same absorbance values at 275 nm, the relative emission intensities for 1:2 at 976 nm in MeCN was 2.70 under the same experimental conditions. This observation supports the idea that the helical ligand framework in **1** provides improved shielding of Yb(III) ions vs those in **2**.

Conclusions

The solid-state structure of the triple-decker Schiff base complex [Yb$_3$L$_3$(OAc)$_2$Cl] (**1**) reveals a complex supramolecular architecture involving cross-linked 1-D stands of molecules linked by $\pi-\pi$ stacking and hydrogen-bonded interactions. Studies suggest that the π-stacked helical triple-decker configuration of salen ligands around the Yb$_3$ core provides superior photoemissive properties compared to those of a single heterodinuclear YbZnL type complex.

Supporting Information Available: Views of the supramolecular structure of [Tb$_3$L$_3$(OAc)$_2$Cl], X-ray crystallographic data as a CIF file. This material is available free of charge via the Internet at http://pubs.acs.org.

References

(1) (a) McGehee, M. D.; Bergstedt, T.; Zhang, C.; Saab, A. P.; O'Regan, M. B.; Bazan, G. C.; Strdanov, V. I.; Heeger, A. *J. Adv. Mater.* **1999**, *11*, 1349. (b) Lehn, J.-M. *Supramolecular Chemistry: Concepts and Perspectives*; VCH: Weinheim, 1995. (c) Piguet, C.; Bünzli, J.-C. G. *Chem. Soc. Rev.* **1999**, *28*, 347. (d) Piguet, C. *Chimia* **1996**, *50*, 144.

(2) (a) Werts, M. H. V.; Hofstraat, J. W.; Geurts, F. A. J.; Verhoeven, J. W. *Chem. Phys. Lett.* **1997**, *276*, 196. (b) Hasegawa, Y.; Ohktbo, T.; Sogabe, K.; Kawamura, Y.; Wada, Y.; Nakashima, H.; Yanagida, S. *Angew. Chem.* **2000**, *112*, 365. Hasegawa, Y.; Ohktbo, T.; Sogabe, K.; Kawamura, Y.; Wada, Y.; Nakashima, H.; Yanagida, S. *Angew. Chem., Int. Ed.* **2000**, *39*, 357.

(3) (a) Sabbatini, N.; Guardigli, M.; Lehn, J. M. *Coord. Chem. Rev.* **1993**, *123*, 201. (b) Alison, S. G.-P.; Ishenkumba, A. K.; Andrew, J. P. W.; David, J. W. *Inorg. Chem.* **1999**, *38*, 1745. (c) Peter, L. J.; Angelo, J. A.; John, C. J.; Jon, A. M.; Elefteria, P.; Leigh, H. R.; Michael, D. W. *Inorg. Chem.* **1997**, *36*, 10. (d) Ohash, K.; Yoshikawa, S.; Akutsu, B.; Nakano, Y.; Usui, Y. *Anal. Sci.* **1990**, *6*, 7. (e) Alpha, B.; Lehn, J.-M.; Mathis, G. *Angew. Chem., Int. Ed. Engl.* **1987**, *26*, 266.

(4) Yang, X.-P.; Jones, R. A. *J. Am. Chem. Soc.*, **2005**, *127*, 7686.

(5) (a) Wong, W.-K.; Liang, H.; Wong, W.-Y.; Cai, Z.; Li, K.-F.; Cheah, K.-W. *New J. Chem.* **2002**, *26*, 275. (b) Lo, W.-K.; Wong, W.-K.; Guo, J.-P.; Wang, W.-Y.; Li, K.-F.; Cheah, K.-W. *Inorg. Chim. Acta* **2004**, *357*, 4510. (c) Yang, X.-P.; Jones, R. A.; Lynch, V.; Michael, M. O.; Holmes, A. L. *J. Chem. Soc., Dalton Trans.* **2005**, 849.

(6) Sheldrick, G. M. *SHELX 97, A Software Package for the Solution and Refinement of X-ray Data*; University of Göttingen: Göttingen, Germany, 1997.

(7) Cromer, D. T.; Waber, J. T. *International Tables for X-ray Crystallography*; Kynoch Press: Birmingham, 1974; Vol. 4, Table 2.2A.

CG0603319